Health and Safety

R94/242

DL/SCI/TM102A

technical memorandum Daresbury Laboratory

DL/SCI/TM102

LENDING COPY

HEALTH PHYSICS EXPERIENCE AROUND SYNCHROTRON RADIATION BEAMLINES

by

R. RYDER and M.P. HOLBOURN, DRAL Daresbury Laboratory

June, 1994

94/524

DRAL
Daresbury Laboratory
Rutherford Appleton Laboratory
DRAL is part of the Engineering and Physical Sciences Research Council

Daresbury Laborato
Daresb
Warring
Chest
WA4 4.

ISSN 0144-5677

HEALTH PHYSICS EXPERIENCE AROUND SYNCHROTRON RADIATION BEAMLINES

R Ryder and M P Holbourn, DRAL[†], EPSRC

ABSTRACT

Many electron storage rings are under construction world wide for use as synchrotron radiation facilities. Very little information has been published to help health physicists design and test synchrotron radiation beamlines. Practical advice is given.

The operational health physics problems around the SRS beamlines at Daresbury Laboratory England, for the past ten years, and more recently at the ESRF Grenoble, are discussed. Guidance for the design of beamlines and shutters is given for radiation of characteristic energy from 4 to 100 keV. Guidance for the design of hutches including shielding joints and service labyrinths is given. Shielding for gas bremsstrahlung is described.

The energy response curves for the portable x-ray monitors used are compared with the scattered synchrotron radiation spectra from SRS dipole and wiggler beamlines.

† Daresbury Rutherford Appleton Laboratories, Daresbury Laboratory, Daresbury, Warrington, Cheshire, UK, WA4 4AD.

1. INTRODUCTION

Synchrotron radiation is produced by bending relativistic electrons (or positrons) in a magnetic field. The energy spectrum of synchrotron radiation extends from the infra red, through the visible and ultra-violet, to the x-ray region. Synchrotron radiation is widely used in biological and medical research, material science, chemistry, lithography and metallurgy. The Synchrotron Radiation Source at Daresbury in the UK has been operational since 1981 and the ESRF at Grenoble was commissioned last year. Other sources are being commissioned at Triesti, Argonne and LBL.

The characteristic energy (E_c) of the spectrum can be used to denote the hardness of the x-rays. The characteristic energy bisects the power distribution of the spectrum and is given by

$$E_c = 0.667BE^2 \text{ KeV} \quad \text{where} \quad B = \text{magnetic field in Tesla}, \quad E = \text{electron energy in GeV}$$

High field magnets are used in insertion devices known as wigglers and many pole magnets are known as undulators. Wiggler magnets are used to increase the radiated power and to extend the energy of the x-rays. Undulator magnets may also be used to increase the radiated power and can be used to tune the radiation to a particular energy. The characteristic energy, and the radiated power and dose rate in the x-ray beams at the SRS and ESRF, for their nominal currents of 320 mA and 150 mA respectively, are listed in Table 1 below. The dose rate in the beam absorbed within the first 10 mm of tissue is calculated using the program PHOTON[1] at 10 m from the source point.

Table 1. Source Characteristics

Beam line	Energy (GeV)	Field (T)	E_c (keV)	Power ($W/mrad_h$)	Dose rate ($Gy\ h^{-1}$)
SRS dipole	2.00	1.20	3.20	10.70	5.98×10^8
wiggler 1	2.00	5.00	13.30	155.20	3.28×10^9
wiggler 2	2.00	6.00	16.00	186.90	3.29×10^9
ESRF dipole	6.00	0.85	20.40	87.50	4.63×10^9
ID17	6.00	1.80	43.20	3370.00	7.81×10^{10}
ID15S	6.00	4.00	96.10	1221.00	1.13×10^{10}

2. HIGH ENERGY RADIATION

Although electron beam lifetimes are generally between 10 and 45 hours, electrons are still lost from the stored beam. The lifetime of the beam is limited by the vacuum at high currents. Electrons are lost from the beam mainly by bremsstrahlung interactions with residual gas molecules. These gas bremsstrahlung photons are highly energetic, with a maximum energy corresponding to the electron energy, and will pass down the beamline. If an electron loses only a small fraction of it's energy when scattering, the energy loss may be compensated for by the RF power in the next cavity it passes and remain within the beam envelope. Electrons whose energy loss cannot be made up by the cavities will be lost from the beam and strike the inside of the vacuum vessel further downstream, producing an electromagnetic cascade of high energy photons.

2.1 HIGH ENERGY CASCADE PHOTONS

This radiation has a wide angular distribution. For beamlines originating at a dipole (bending) magnet with an angular acceptance of less than 40 mradians, a series of collimators can be used to prevent radiation passing down the line. For maximum efficiency, the first collimator should be located in the exit arm of the dipole vacuum vessel. Figure 1 shows a typical arrangement for dipole beamlines at the SRS. Maximum access to the beamline is guaranteed by this arrangement.

For beamlines which originate at straight sections or have an angular acceptance greater than 40 mradians, collimation is not totally effective and the line must either be shielded or be provided with restricted access enclosures.

2.2 GAS BREMSSTRAHLUNG

The production of high energy bremsstrahlung radiation due to the interaction of the stored electron beam with the residual gas molecules in electron storage rings is a well known problem. This can be a significant source of radiation in today's machines where the magnet lattice straight sections are particularly long to allow the insertion of multipole wiggler and undulator devices.

The bremsstrahlung photons are emitted in a narrow cone with a characteristic half angle of $\frac{E}{m_o c^2}$ milliradians, where E is the electron energy in GeV. For beamlines originating from dipole magnets the bremsstrahlung can be considered to be a point source located on the tangent with a rectangular profile. The height is defined by the characteristic opening angle of the radiation with the width equal to that accepted by the beamline collimator. For beamlines originating from long straight sections the bremsstrahlung can be treated as an extended source viewed on axis with a circular profile.

A review of the literature reveals a variety of formulae for the magnitude of the gas bremsstrahlung dose rate derived either from bremsstrahlung theory[2,3] or using Monte Carlo techniques.[4,5] These expressions have been rationalised to take into account the variation in units and are given below.

Ref. 2 $$D_d = \frac{8.0\text{x}10^{-7}\, PIE_o^2 l}{X_o d^2} \quad \mu\text{Gy h}^{-1}$$

Ref. 3 $$D_d = \frac{4.49\text{x}10^{-7}\, PIE_o^2 l}{X_o d(l+d)} \quad \mu\text{Gy h}^{-1}$$

Ref. 4 $$D_d = 2.24\text{x}10^{-13}\, PIE_o^{2.43} l \left(\frac{10+l/2}{d}\right)^2 \quad \mu\text{Gy h}^{-1}$$

Ref. 5 $$D_d = \frac{1.5\text{x}10^{-11}\, PIE_o^{2.67} l}{d(l+d)} \quad \mu\text{Gy h}^{-1}$$

where P= vacuum pressure at origin of beamline in torr
I = ring current in electrons per sec
E= electron energy in MeV
l = length of gas target in m
d= distance from origin in m

Figure 2 shows a plot of these expressions for the case of an ESRF straight section. There is considerable variation across the curves particularly at distances close to the end of the straight. This is due to the geometry of the situation considered in each case and the method used to correct for viewing an extended source on axis. All methods are in good agreement at distances greater than about 20 m given the variation in radiation length assumed for the residual gas. Holbourn[2] uses a length of 568 m by considering the residual gas to be 60% CO and 40% H_2. A figure of 308 m is used by Bräuer[6] which is more representative of air. The variation in the energy term is due to the difference in flux to dcse conversion coefficients considered. Holbourn[2] uses a figure of 5.0 μGy h^{-1}/cm^2s^{-1} proposed by Tesch[7] while both Tromba and Rindi[4] and Ferrari *et al*[5] use the energy dependant fluence to dose conversions from Rogers.[8] Figure 3 shows the requirements for stopping the primary bremsstrahlung beam, from an ESRF straight, in lead. The curves represent the four equations above. An attenuation of 50 m^{-1} for lead is used although Tromba and Rindi[4] recommend a value of 60 m^{-1} from their Monte Carlo calculations.

Measurements have been made at the ESRF on beamline ID9 of the magnitude of the scattered gas bremsstrahlung from two different thickness beam stops. Figures 4(a) and 4(b) show the measured vertical and horizontal profiles of the scattered bremsstrahlung across the rear wall of the experimental hutch 50 m from the centre of the straight. Figure 5 shows the scattered dose rate as a function of angle across the rear wall. This decrease in dose rate in angle is much less than that expected from the Monte Carlo calculations of Ipe *et al.*[9]

3. SYNCHROTRON RADIATION

The spectra of various beamlines at the SRS and ESRF are shown in Figure 6. These spectra have been calculated using the PHOTON code. This code uses the bending magnet approximation for multipole magnets and hence progressively overestimates the photon flux at higher energies. There is a wide variation in the characteristic energy of the spectra from these sources, however the dose rate in the beam for all cases are in excess of 10^8Gy h^{-1}. More than 14 TVLs are therefore required to reduce the dose rates to permitted levels. The characteristic energy is important in the choice of shield material for the experimental enclosures, known as hutches, needed where the x-ray beam is allowed to emerge into air.

3.1 HUTCH SHIELDING DESIGN

For beamlines whose characteristic energy is below 5 keV, steel shielding is most economical and there are no special problems associated with the fabrication of steel hutches. The vacuum pipes and other components are made from 3 mm thick steel. Occasionally small dose rates of x-rays emerge from thin vacuum bellows and thin welded seams. These are easily shielded by wrapping 1 mm lead sheet around the area. Figure 7 shows the method of construction for the x-ray hutches on the dipole radiation lines at the SRS.

Beamlines with x-rays whose characteristic energy is above 5 keV are normally shielded with lead and great care is needed in the design of the hutches to ensure that x-ray penetration of the hutch fabric is not a problem. The walls must be grouted to the floor with lead loaded grout or a lead apron provided to prevent x-rays passing between the walls and the floor. It is important to have lead to lead overlaps rather than butt joints. The lead panels must be attached to the frame work by bolts covered by a lead strip. Three methods of construction of lead hutches have been used at the SRS and ESRF.

The method adopted by Fabcast† (Figure 8) at the SRS and ESRF of a plywood, lead, plywood sandwich screwed to steel box members has worked well for radiation up to 20 keV characteristic energy. The panels are fabricated to a size which a man can lift. A lead cover strip is glued over the joints. The plywood facing can be used to support other equipment provided the screws do not penetrate the lead. This method fabrication is labour intensive but has the advantage that it is easily modified. It is likely that the Fabcast method will be chosen for the hutches on the ESRF 'super-wiggler' which will produce radiation with a characteristic energy of 96 keV.

The Antitron†† construction method of a steel, lead, steel sandwich bolted to steel beams (Figure 9) has been used at the ESRF for radiation of characteristic energy up to 36 keV. The panels are a fixed size of 2 x 1 m^2 and require a crane to lift them. The cover strip over the joints is narrow and x-rays can pass around them. X-rays have also penetrated the shield through the bolts holding the panels to the support frame. The lead loaded resin caps covering the head of the bolts are not entirely effective and are prone to getting displaced or lost.

The method of construction adopted by Ferraro††† is shown in Figure 10. The lead is sandwiched between layers of polyurethane foam with an outer skin of 1 mm steel sheet. Each panel consists of 2 sheets of lead which interleave with the next panel. Each panel is 5 m tall by 1 m wide. Two of these panels are joined together on the floor before being craned to the vertical. The panels are

† Fabcast Engineering Ltd, Unit G4, Riverside Industrial Estate, Riverside Way, Dartford, United Kingdom, DA1 5BJ, Tel: 0322 222 262

†† Antitron, Kastanien. 12, D6230, Frankfurt / M80, Germany. Tel: 010 49 693 872 14

††† Ferraro, Via Brigate, Tarteigiane 2, 17014 Tiro Montenotte, Savona, Italy. Tel: 010 39 195 010 62

bolted onto a steel frame using a minimum number of bolts. Again x-rays penetrate the bolts. The foam cladding provides some rigidity and insulation but the panels are not load bearing and tend to flex, particularly on the roof. However this method of construction is relatively light and easy to construct.

Doors and door frames which provide an x-ray tight seal are particularly difficult to design. The higher the characteristic energy and the dose rate in the beam, the greater the problems. The foot of the door must seal against a door sill. The gap between the door and frame should be minimised. Care in minimising manufacturing tolerances and quality of fabrication are important. Door seals which rely solely on lead to lead contact are rarely effective. Door seals should be designed so that x-rays undergo either a 180° or two 90° scatters.

Many pipes and cables enter each hutch for cooling water, compressed air, counting gas, power supplies and detector signal cables. These sevices enter through labyrinths. As the required aperture through the hutch wall or roof can be large, particularly in the case of air conditioning and ozone extraction systems, a lot of care is required to prevent significant doses of x-rays passing down the labyrinth. The design criteria for hutches accepting radiation with characteristic energy below and above 5 keV is shown in Figures 11(a) and 11(b). This method of construction has proved effective on the SRS dipole and wiggler hutches.

3.2 MONITORING X-RAYS

Most x-rays penetrating the hutch walls and labyrinths will have undergone at least one scatter from some object such as a monochromator or focusing mirror. The x-ray spectra from SRS dipole and 6 T wiggler beams scattered from a copper block 25 mm thick, representing the backing of a mirror, are shown in Figure 12. At the SRS, Mini Instruments† monitors type 900X are used to monitor x-rays around the beam lines. This monitor uses an un-compensated Philips GM detector, type ZP1481, with a thin mica window. It's response as a function of energy is shown in Figure 12. The monitor has a semi-logarithmic meter scaled in counts per sec. The response of a Mini Instruments monitor type 900D which uses a Philips compensated GM detector type ZP1490 is shown for comparison. It is calibrated in $\mu Sv\ h^{-1}$.

† Mini Instruments Ltd. 6 Station Industrial Estate, Burnham-on-Crouch, Essex, United Kingdom, CM0 8RN. Tel: 0621 783 282

The compensated GM detector will not respond to the contribution of X-rays below 30 keV and hence considerably underestimates the x-ray dose rate. The un-compensated GM detector responds down to 4 keV. It misses only a small fraction of the low energy x-rays. The over estimation of the contribution above 10 keV more than compensates for this loss. The monitor therefore overestimates the true dose rate.

At the ESRF, a temporary beryllium window, enclosed in an inert atmosphere of nitrogen and mylar window is provided to allow all hutches to be tested with beam before any experimental equipment is installed in the hutch. A cooled absorber is used as a scatterer at various positions in the hutch to check each door and window.

4. CONCLUSION

The use of collimators to reduce gas bremsstrahlung on dipole beamlines is described. The first collimator should be positioned inside the vacuum vessel for maximum efficiency. Although the various formulations for dose rate due to gas bremsstrahlung show a difference of up to a factor of 5 at distances below 20 m from the origin, this is rarely a problem. The various formulas and attenuation coefficients proposed by several authors results in only a 10 % difference in the thickness of beam stops. Three different hutch designs are shown and their merits and disadvantages are discussed. The importance of using an un-compensated GM detector for monitoring around the hutch and beamlines is emphasised.

5. ACKNOWLEDGEMENT

The authors are grateful to Paul Berkvens of the ESRF who provided the opportunity to participate in the work of the ESRF Health Physics Section whilst commissioning the new beamlines.

6. REFERENCES

1. Chapman D. PHOTON: A Users Manual. Brookhaven National Laboratory internal report BNL40822

2. Holbourn M.P. Gas Bremsstrahlung Production in the SRS. Health Physics Report HP81/139, 1981

3. Esposito A. and Pelliccioni M. Gas Bremsstrahlung Production in the Adone Storage Ring. LNF-86/23(NT), 1986

4. Tromba G. and Rindi A. Gas Bremsstrahlung from Electron Storage Rings. A Monte Carlo Evaluation and Some Useful Formula. Nuclear Instruments and Methods in Physics Research, A292, 1990

5. Ferrari A., Pelliccioni M. and Sala P.R. Estimation of Fluence Rate and Absorbed Dose Rate Due to Gas Bremsstrahlung from Electron Storage Rings. LNF-93/016(P), 1993

6. Bräuer E. Health Physics Measurements around the new F2 Wiggler Station at CHESS. ESRF Internal Report.

7. Tesch K. Nukleonik. Vol 8, 1966.

8. Rogers D.W.O. Health Physics, Vol 46, 1984

9. Ipe N.E., Haeffner D.R., Alp E.E., Davey S.C., Dejus R.J., Hahn U., Lai B., Randall K.J. and Shu D. Guide to Beamline Radiation Shielding at the Advanced Photon Source. SLAC TN 93-5.

Figure 1. Layout of lead collimators for SRS dipole beamlines.

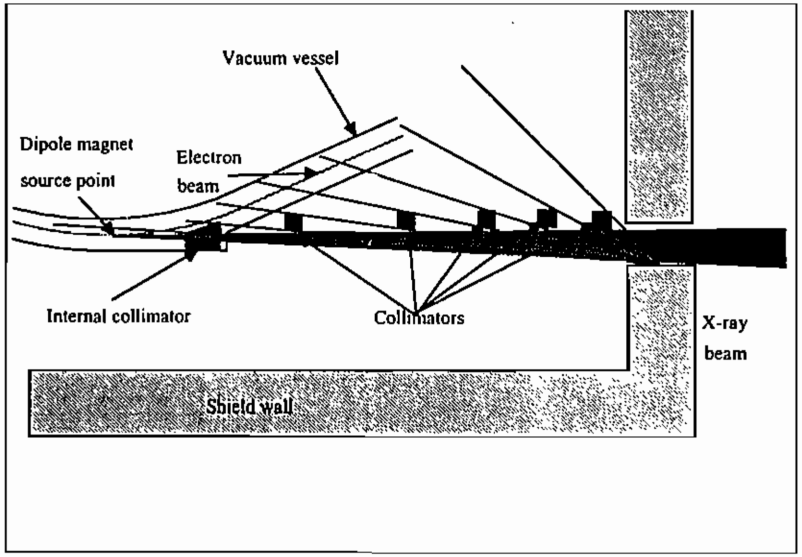

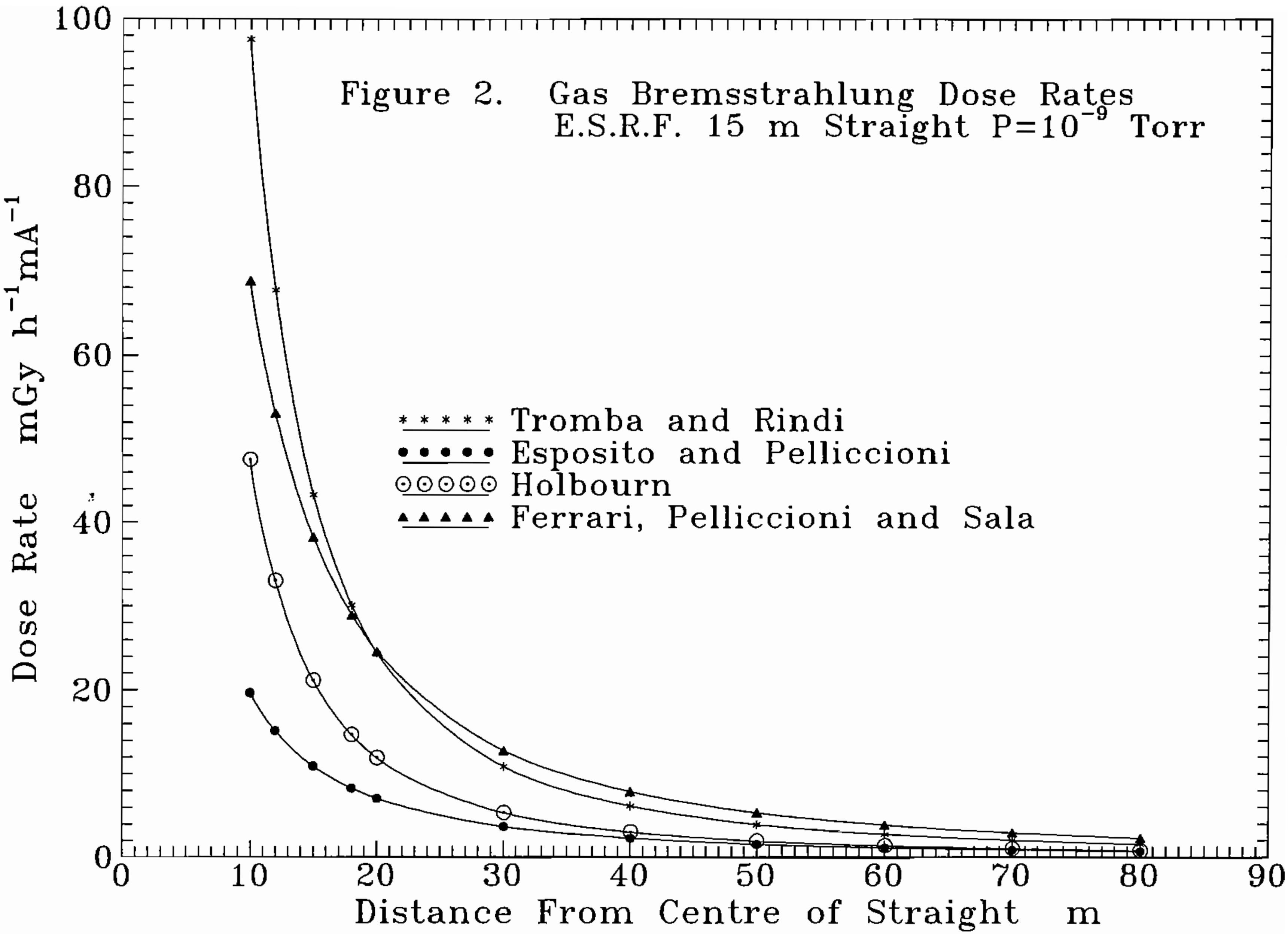

Figure 2. Gas Bremsstrahlung Dose Rates
E.S.R.F. 15 m Straight P=10^{-9} Torr
Tromba and Rindi
Esposito and Pelliccioni
Holbourn
Ferrari, Pelliccioni and Sala
Dose Rate mGy h^{-1}mA^{-1}
Distance From Centre of Straight m
0
20
40
60
80
100
0
10
20
30
40
50
60
70
80
90

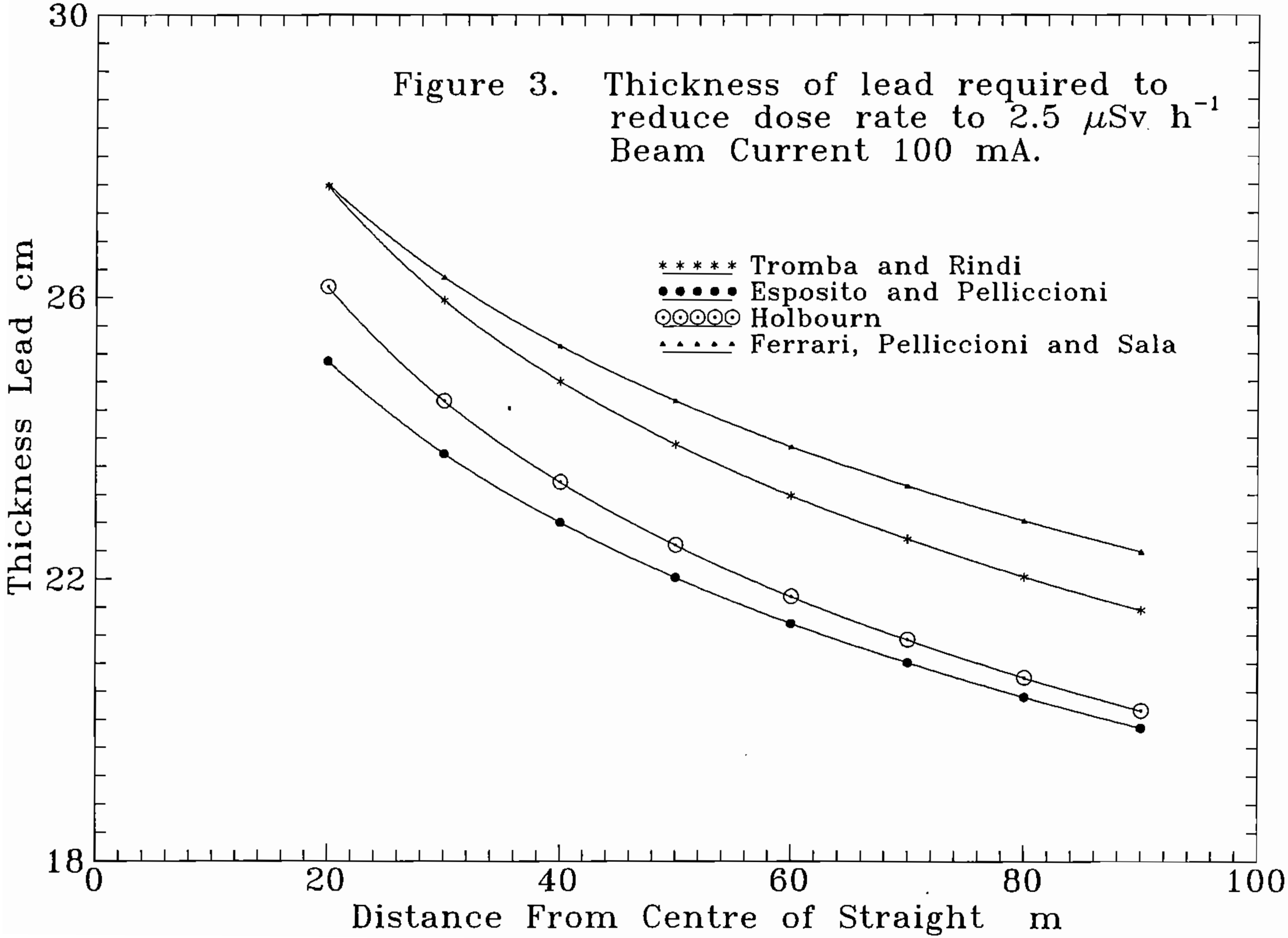
Figure 3. Thickness of lead required to reduce dose rate to 2.5 μSv h^{-1} Beam Current 100 mA.
Tromba and Rindi
Esposito and Pellicciorni
Holbourn
Ferrari, Pellicciorni and Sala
Thickness Lead cm
30
26
22
18
0
20
40
60
80
100
Distance From Centre of Straight m

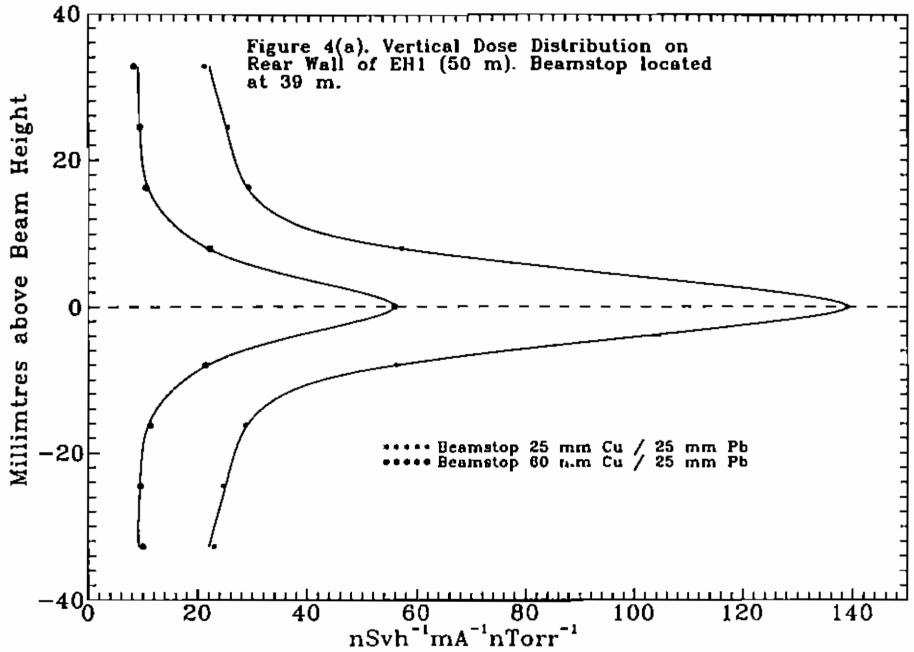
Figure 4(a). Vertical Dose Distribution on Rear Wall of EH1 (50 m). Beamstop located at 39 m.
Millimetres above Beam Height
nSvh⁻¹mA⁻¹nTorr⁻¹
Beamstop 25 mm Cu / 25 mm Pb
Beamstop 60 mm Cu / 25 mm Pb
40
20
0
−20
−40
0
20
40
60
80
100
120
140

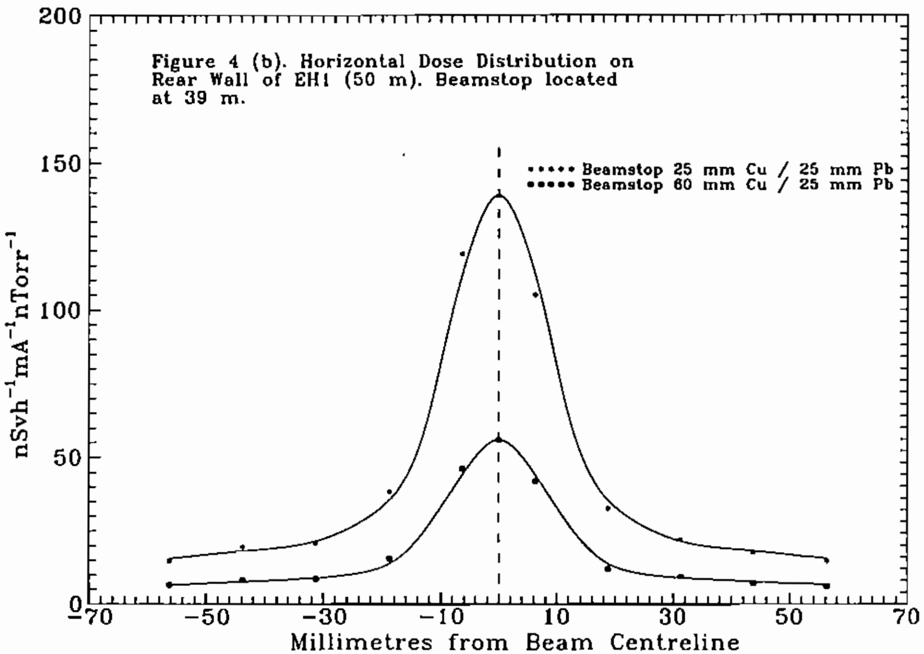
Figure 4 (b). Horizontal Dose Distribution on Rear Wall of EH1 (50 m). Beamstop located at 39 m.
nSvh⁻¹mA⁻¹nTorr⁻¹
Millimetres from Beam Centreline
Beamstop 25 mm Cu / 25 mm Pb
Beamstop 60 mm Cu / 25 mm Pb
200
150
100
50
0
−70
−50
−30
−10
10
30
50
70

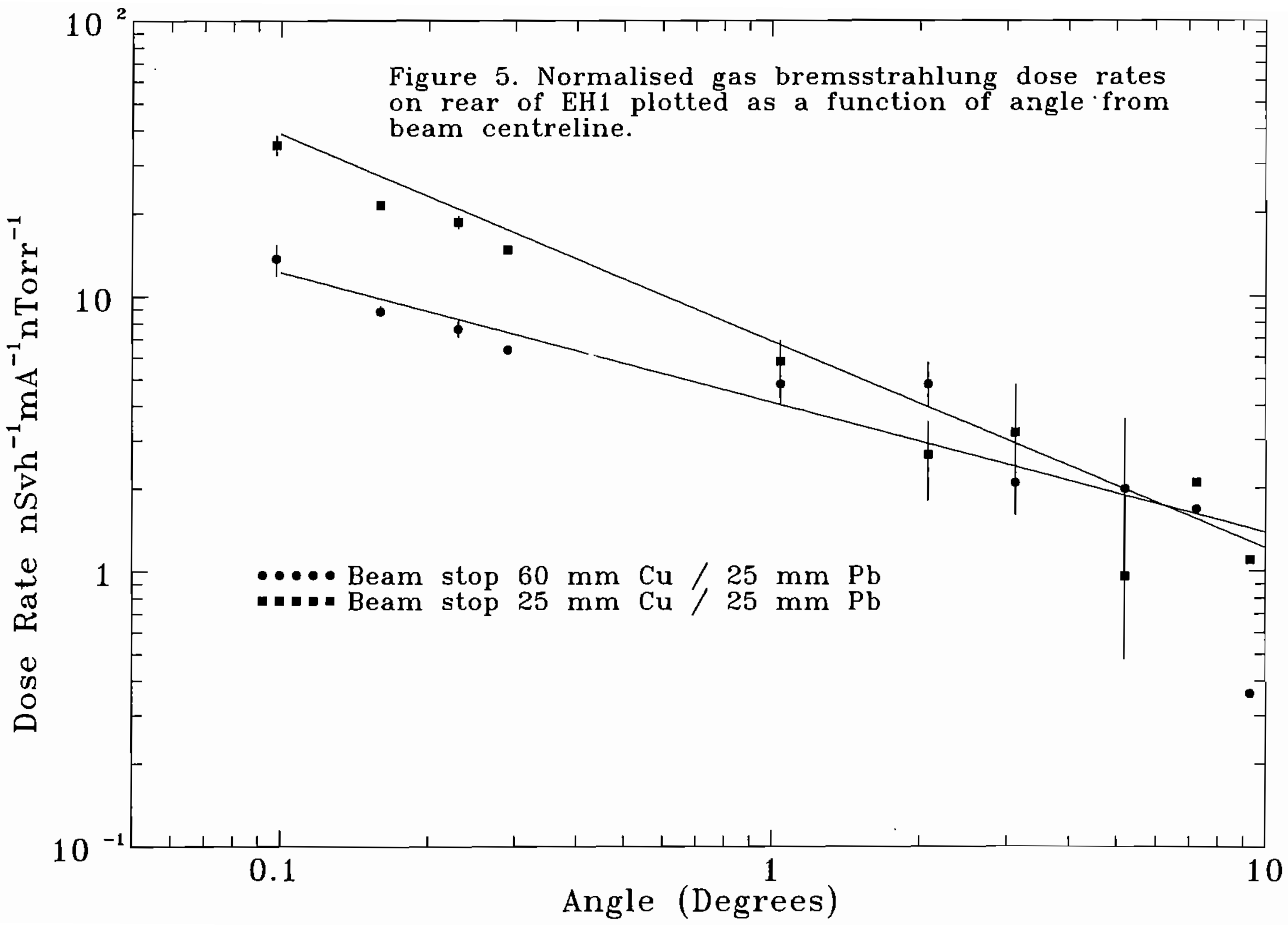

Figure 5. Normalised gas bremsstrahlung dose rates on rear of EH1 plotted as a function of angle from beam centreline.
Beam stop 60 mm Cu / 25 mm Pb
Beam stop 25 mm Cu / 25 mm Pb
Dose Rate nSvh⁻¹mA⁻¹nTorr⁻¹
Angle (Degrees)
10²
10
1
10⁻¹
0.1
1
10

Figure 6. X-ray Spectra of some SRS and ESRF beamlines

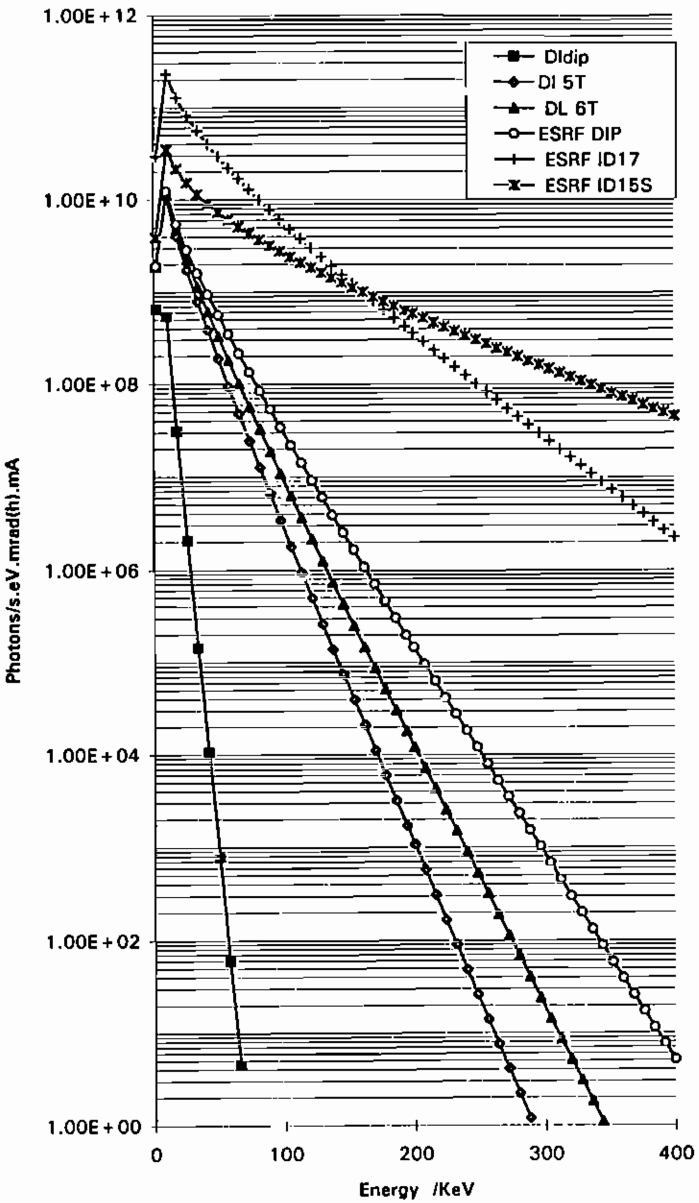

Figure 7. Construction detail of SRS dipole hutches.

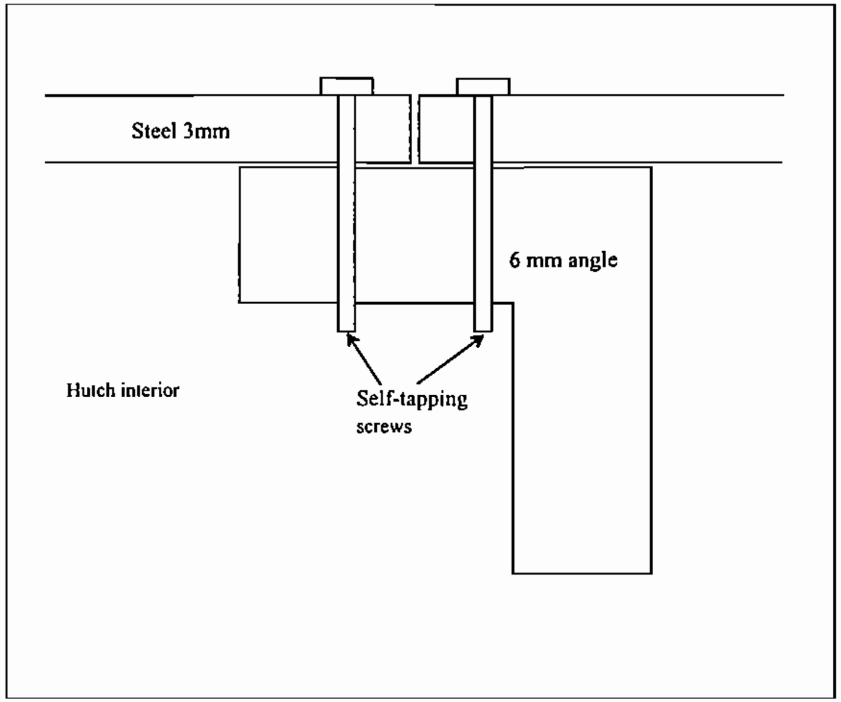

Figure 8. Design of the wall joints in the Fabcast Hutches.

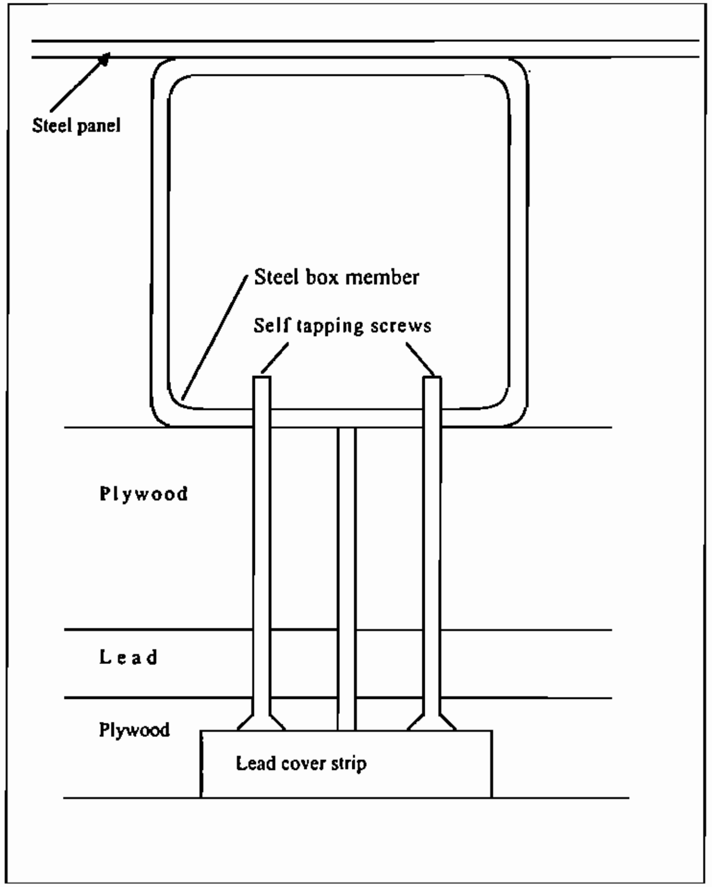

Figure 9. Antitron design of wall panel joint.

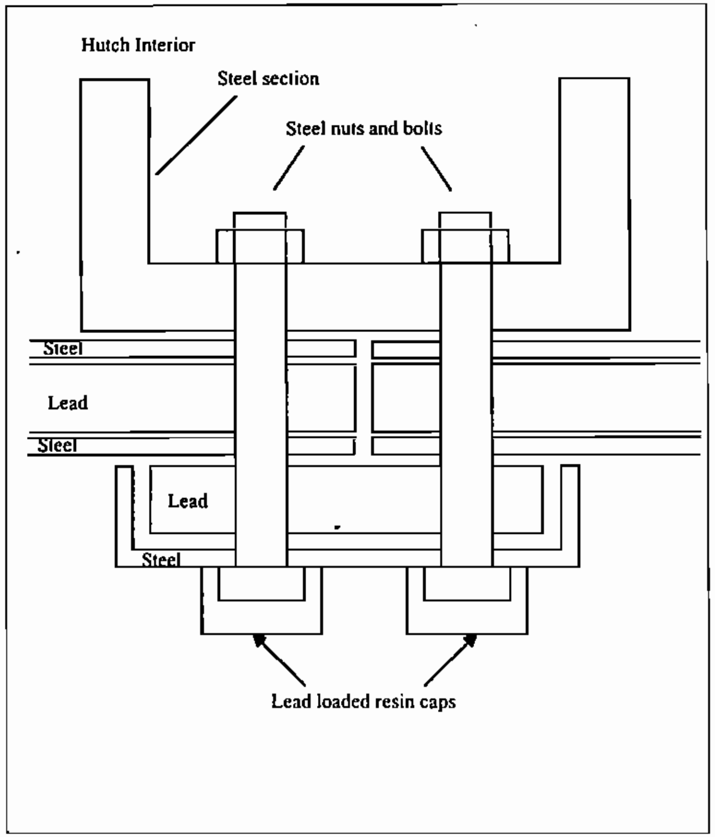

Figure 10. Design of wall joint used by Ferraro

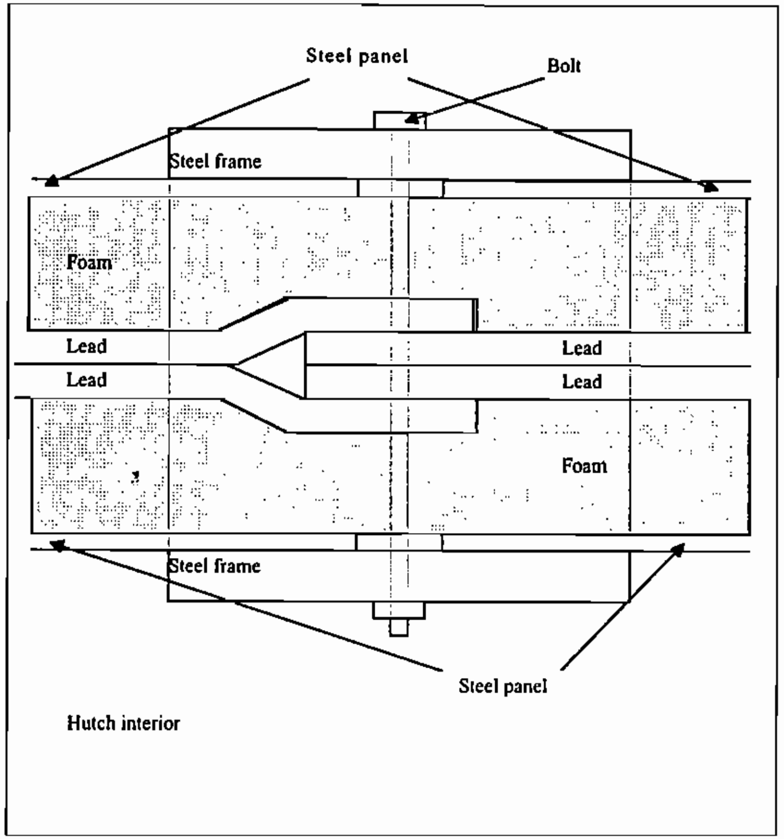

Figure 11a. SRS dipole hutch services entry labyrinth.

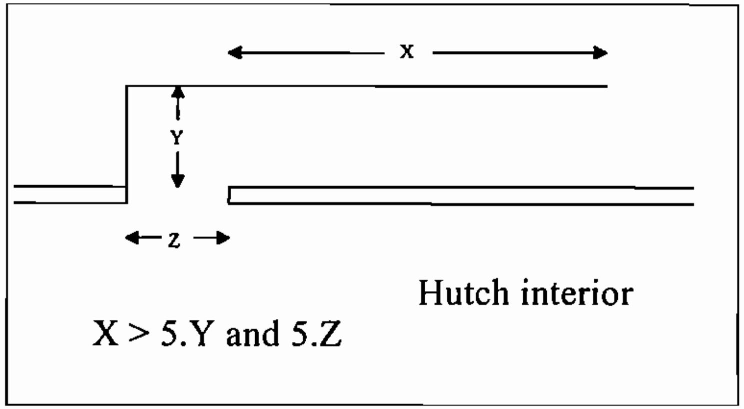

Figure 11b. SRS wiggler hutch services entry labyrinth.

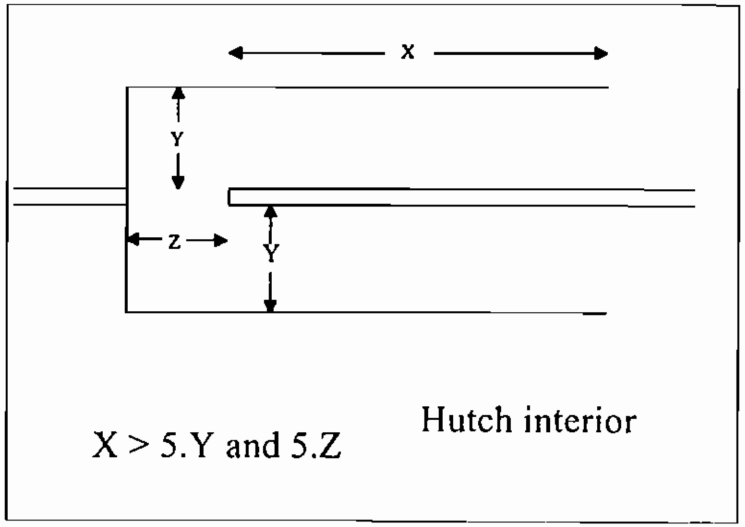

Figure 12. Comparison of monitor responses and energy spectra.